International Telecommunication Union

ITU-R

Radiocommunication Sector of ITU

Recommendation ITU-R P.1411-7
(09/2013)

Propagation data and prediction methods for the planning of short-range outdoor radiocommunication systems and radio local area networks in the frequency range 300 MHz to 100 GHz

P Series

Radiowave propagation

International Telecommunication Union

Foreword

The role of the Radiocommunication Sector is to ensure the rational, equitable, efficient and economical use of the radio-frequency spectrum by all radiocommunication services, including satellite services, and carry out studies without limit of frequency range on the basis of which Recommendations are adopted.

The regulatory and policy functions of the Radiocommunication Sector are performed by World and Regional Radiocommunication Conferences and Radiocommunication Assemblies supported by Study Groups.

Policy on Intellectual Property Right (IPR)

ITU-R policy on IPR is described in the Common Patent Policy for ITU-T/ITU-R/ISO/IEC referenced in Annex 1 of Resolution ITU-R 1. Forms to be used for the submission of patent statements and licensing declarations by patent holders are available from http://www.itu.int/ITU-R/go/patents/en where the Guidelines for Implementation of the Common Patent Policy for ITU-T/ITU-R/ISO/IEC and the ITU-R patent information database can also be found.

Series of ITU-R Recommendations

(Also available online at http://www.itu.int/publ/R-REC/en)

Series	Title
BO	Satellite delivery
BR	Recording for production, archival and play-out; film for television
BS	Broadcasting service (sound)
BT	Broadcasting service (television)
F	Fixed service
M	Mobile, radiodetermination, amateur and related satellite services
P	**Radiowave propagation**
RA	Radio astronomy
RS	Remote sensing systems
S	Fixed-satellite service
SA	Space applications and meteorology
SF	Frequency sharing and coordination between fixed-satellite and fixed service systems
SM	Spectrum management
SNG	Satellite news gathering
TF	Time signals and frequency standards emissions
V	Vocabulary and related subjects

Note*: This ITU-R Recommendation was approved in English under the procedure detailed in Resolution ITU-R 1.*

Electronic Publication
Geneva, 2013

RECOMMENDATION ITU-R P.1411-7

Propagation data and prediction methods for the planning of short-range outdoor radiocommunication systems and radio local area networks in the frequency range 300 MHz to 100 GHz

(Question ITU-R 211/3)

(1999-2001-2003-2005-2007-2009-2012-2013)

Scope

This Recommendation provides guidance on outdoor short-range propagation over the frequency range 300 MHz to 100 GHz. Information is given on path loss models for line-of-sight (LoS) and non-line-of-sight (NLoS) environments, building entry loss, multipath models for both environments of street canyon and over roof-tops, number of signal components, polarization characteristics and fading characteristics.

The ITU Radiocommunication Assembly,

considering

a) that many new short-range (operating range less than 1 km) mobile and personal communication applications are being developed;

b) that there is a high demand for radio local area networks (RLANs) and wireless local loop systems;

c) that short-range systems using very low power have many advantages for providing services in the mobile and wireless local loop environment;

d) that knowledge of the propagation characteristics and the interference arising from multiple users in the same area is critical to the efficient design of systems;

e) that there is a need both for general (i.e. site-independent) models and advice for initial system planning and interference assessment, and for deterministic (or site-specific) models for some detailed evaluations,

noting

a) that Recommendation ITU-R P.1238 provides guidance on indoor propagation over the frequency range 900 MHz to 100 GHz, and should be consulted for those situations where both indoor and outdoor conditions exist;

b) that Recommendation ITU-R P.1546 provides guidance on propagation for systems that operate over distances of 1 km and greater, and over the frequency range 30 MHz to 3 GHz,

recommends

that the information and methods in Annex 1 should be adopted for the assessment of the propagation characteristics of short-range outdoor radio systems between 300 MHz and 100 GHz where applicable.

Annex 1

1 Introduction

Propagation over paths of length less than 1 km is affected primarily by buildings and trees, rather than by variations in ground elevation. The effect of buildings is predominant, since most short-path radio links are found in urban and suburban areas. The mobile terminal is most likely to be held by a pedestrian or located in a vehicle.

This Recommendation defines categories for short propagation paths, and provides methods for estimating path loss, delay spread, angular spread, and cross correlation over these paths.

The propagation models of these methods are symmetric in the sense that they treat radio terminals at both ends of a path in the same manner. From the model's perspective, it does not matter which terminal is the transmitter and which is the receiver. Hence the terms "Station 1" and "Station 2" are used to denote the terminals at the start and end of the propagation path, respectively.

2 Physical operating environments and definition of cell types

Environments described in this Recommendation are categorized solely from the radio propagation perspective. Radiowave propagation is influenced by the environment, i.e. building structures and heights, the usage of the mobile terminal (pedestrian/vehicular) and the positions of the antennas. Five different environments are identified, considered to be the most typical. Hilly areas, for example, are not considered, as they are less typical in metropolitan areas. Table 1 lists the five environments. Recognizing that there is a wide variety of environments within each category, it is not intended to model every possible case but to give propagation models that are representative of environments frequently encountered.

TABLE 1

Physical operating environments – Propagation impairments

Environment	Description and propagation impairments of concern
Urban very high-rise	– Busiest urban deep canyon, characterized by streets lined with high-density buildings with several tens of floors which results in an urban deep canyon – High dense buildings and skyscrapers interleave with each other which yields to the rich scattering propagation paths in NLoS – Rows of tall buildings provide the possibility of very long path delays – Heavy traffic vehicles and high flowrate visitors in the area act as reflectors adding Doppler shift to the reflected waves – Trees beside the streets provide dynamic shadowing
Urban high-rise	– Urban canyon, characterized by streets lined with tall buildings of several floors each – Building height makes significant contributions from propagation over roof-tops unlikely – Rows of tall buildings provide the possibility of long path delays – Large numbers of moving vehicles in the area act as reflectors adding Doppler shift to the reflected waves

TABLE 1 (*end*)

Environment	Description and propagation impairments of concern
Urban low-rise/Suburban	– Typified by wide streets – Building heights are generally less than three stories making diffraction over roof-top likely – Reflections and shadowing from moving vehicles can sometimes occur – Primary effects are long delays and small Doppler shifts
Residential	– Single and double storey dwellings – Roads are generally two lanes wide with cars parked along sides – Heavy to light foliage possible – Motor traffic usually light
Rural	– Small houses surrounded by large gardens – Influence of terrain height (topography) – Heavy to light foliage possible – Motor traffic sometimes high

For each of the five different environments two possible scenarios for the mobile are considered. Therefore the users are subdivided into pedestrian and vehicular users. For these two applications the velocity of the mobile is quite different yielding different Doppler shifts. Table 2 shows typical velocities for these scenarios.

TABLE 2

Physical operating environments – Typical mobile velocity

Environment	Velocity for pedestrian users (m/s)	Velocity for vehicular users
Urban very high-rise/Urban high-rise	1.5	Typical downtown speeds around 50 km/h (14 m/s)
Urban low-rise/Suburban	1.5	Around 50 km/h (14 m/s) Expressways up to 100 km/h (28 m/s)
Residential	1.5	Around 40 km/h (11 m/s)
Rural	1.5	80-100 km/h (22-28 m/s)

The type of propagation mechanism that dominates depends also on the height of the base station antenna relative to the surrounding buildings. Table 3 lists the typical cell types relevant for outdoor short-path propagation.

TABLE 3

Definition of cell types

Cell type	Cell radius	Typical position of base station antenna
Micro-cell	0.05 to 1 km	Outdoor; mounted above average roof-top level, heights of some surrounding buildings may be above base station antenna height
Dense urban micro-cell	0.05 to 0.5 km	Outdoor; mounted below average roof-top level
Pico-cell	Up to 50 m	Indoor or outdoor (mounted below roof-top level)

(Note that "dense urban micro-cell" is not explicitly defined in Radiocommunication Study Group 5 Recommendation.)

3 Path categories

3.1 Definition of propagation situations

Three levels of the location of the station can be considered in this Recommendation. They are 1) over the roof-top (designated as L1 in Fig. 1); 2) below roof-top but above head level (L2); and 3) at or below head level (L3). Comprehensively, six different kinds of links can be considered depending on the locations of the stations, each of which may be LoS or NLoS.

Typical propagation situations in urban or suburban areas are depicted in Fig. 1. When one station (A) is mounted above roof-top level and another station (B or C) is located at head level, the corresponding cell is a micro-cell. The path can be LoS (A to C) or NLoS (A to B). The propagation between the stations A and B is mainly over the roof-tops. When one station (D) is mounted below roof-top level but above head level and another station (E or F) is located at head level in an urban or suburban environment, the corresponding cell is a micro- or pico-cellular environment. In these cell types, propagation is mainly within street canyons. For mobile-to-mobile links, both ends of the link can be assumed to be at head level. The path can be LoS (B to E) or NLoS (E to F).

3.1.1 Propagation over rooftops, non-line-of-sight (NLoS)

The typical NLoS case (link A-B in Fig. 1) is described in Fig. 2. In the following, this case is called NLoS1.

FIGURE 1

Typical propagation situation in urban areas

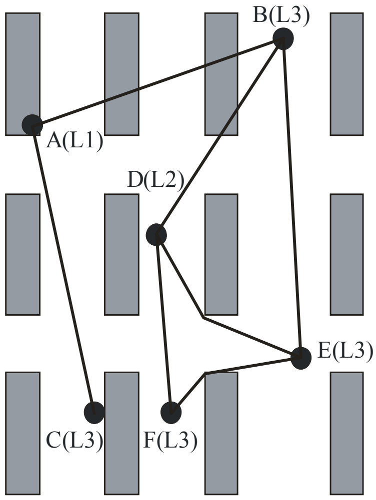

FIGURE 2

Definition of parameters for the NLoS1 case

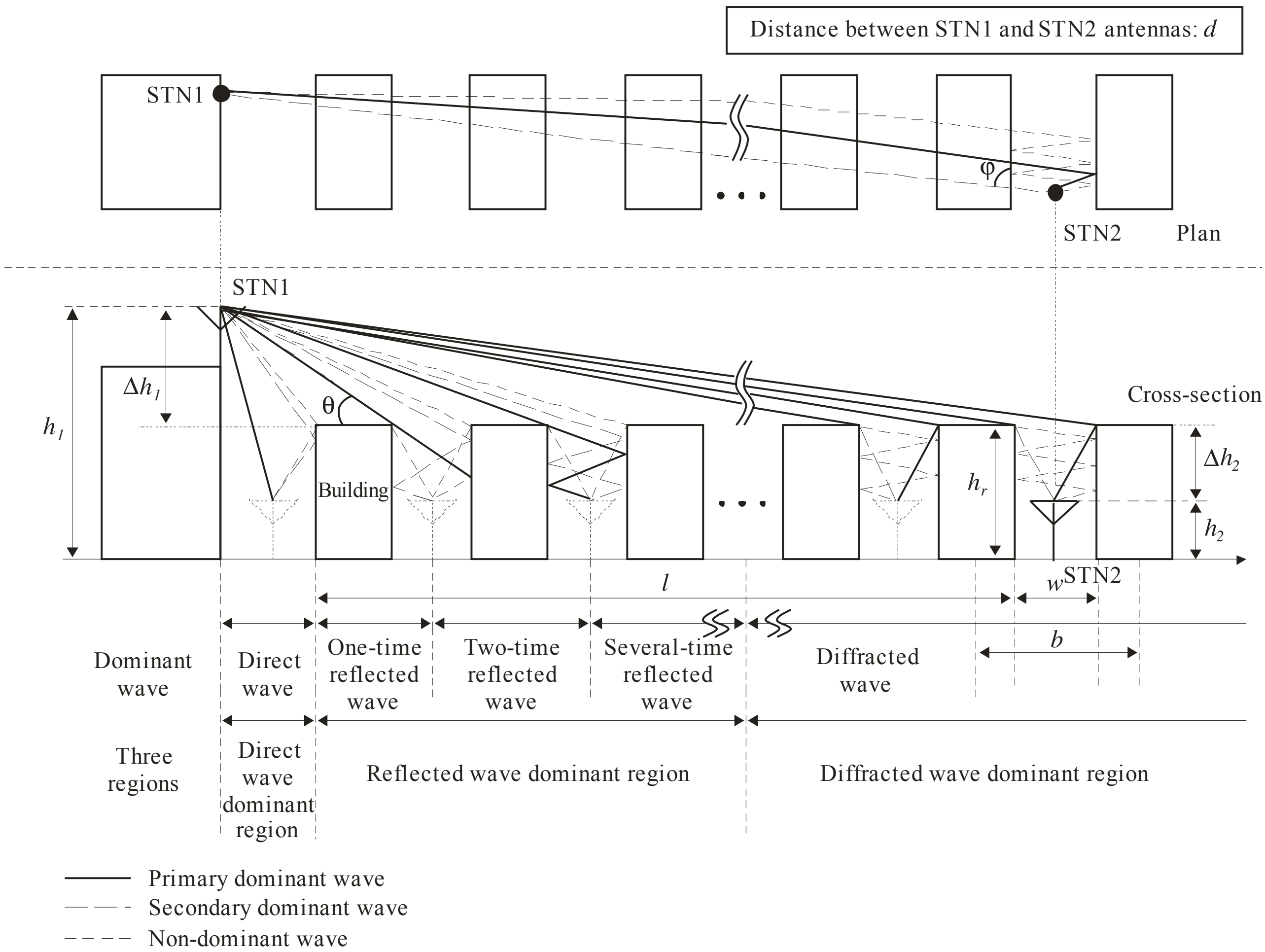

The relevant parameters for this situation are:

h_r: average height of buildings (m)

w: street width (m)

b: average building separation (m)

φ: street orientation with respect to the direct path (degrees)

h_1: Station 1 antenna height (m)

h_2: Station 2 antenna height (m)

l: length of the path covered by buildings (m)

d: distance from Station 1 to Station 2.

The NLoS1 case frequently occurs in residential/rural environments for all cell-types and is predominant for micro-cells in urban low-rise/suburban environments. The parameters h_r, b and l can be derived from building data along the line between the antennas. However, the determination of w and φ requires a two-dimensional analysis of the area around the mobile. Note that l is not necessarily normal to the building orientation.

3.1.2 Propagation along street canyons, NLoS

Figure 3 depicts the situation for a typical dense urban micro-cellular NLoS-case (link D-E in Fig. 1). In the following, this case is called NLoS2.

FIGURE 3

Definition of parameters for the NLoS2 case

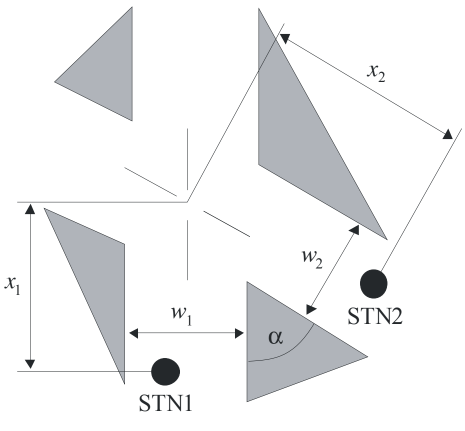

The relevant parameters for this situation are:

w_1: street width at the position of the Station 1 (m)

w_2: street width at the position of the Station 2 (m)

x_1: distance Station 1 to street crossing (m)

x_2: distance Station 2 to street crossing (m)

α: is the corner angle (rad).

NLoS2 is the predominant path type in urban high-rise environments for all cell-types and occurs frequently in dense urban micro- and pico-cells in urban low-rise environments. The determination of all parameters for the NLoS2 case requires a two-dimensional analysis of the area around the mobile.

3.1.3 Line-of-sight (LoS) paths

The paths A-C, D-F, and B-E in Fig. 1 are examples of LoS situations. The same models can be applied for these types of LoS path.

3.2 Data requirements

For site-specific calculations in urban areas, different types of data can be used. The most accurate information can be derived from high-resolution data where information consists of:

– building structures;

– relative and absolute building heights;

– vegetation information.

Data formats can be both raster and vector. The location accuracy of the vector data should be of the order of 1 to 2 m. The recommended resolution for the raster data is 1 to 10 m. The height accuracy for both data formats should be of the order of 1 to 2 m.

If no high-resolution data are available, low-resolution land-use data (50 m resolution) are recommended. Depending on the definition of land-use classes (dense urban, urban, suburban, etc.) the required parameters can be assigned to these land-use classes. These data can be used in conjunction with street vector information in order to extract street orientation angles.

4 Path loss models

For typical scenarios in urban areas, some closed-form algorithms can be applied. These propagation models can be used both for site-specific and site-general calculations. The corresponding propagation situations are defined in § 3.1. The type of the model depends also on the frequency range. Different models have to be applied for UHF propagation and for mm-wave propagation. In the UHF frequency range, LoS and NLoS situations are considered. In mm-wave propagation, LoS is considered only. Additional attenuation by oxygen and hydrometeors has to be considered in the latter frequency range.

4.1 Models for propagation within street canyons

4.1.1 LoS situation

This situation is depicted as the paths between A and C, D and F, or B and E in Fig. 1.

UHF propagation

In the UHF frequency range, basic transmission loss, as defined by Recommendation ITU-R P.341, can be characterized by two slopes and a single breakpoint. An approximate lower bound $L_{LoS,l}$ is given by:

$$L_{LoS,l} = L_{bp} + \begin{cases} 20 \log_{10}\left(\dfrac{d}{R_{bp}}\right) & \text{for} \quad d \le R_{bp} \\ 40 \log_{10}\left(\dfrac{d}{R_{bp}}\right) & \text{for} \quad d > R_{bp} \end{cases} \tag{1}$$

where R_{bp} is the breakpoint distance in m and is given by:

$$R_{bp} \approx \frac{4 h_1 h_2}{\lambda} \tag{2}$$

where λ is the wavelength (m). The lower bound is based on the two-ray plane earth reflection model.

An approximate upper bound $L_{LoS,u}$ is given by:

$$L_{LoS,u} = L_{bp} + 20 + \begin{cases} 25 \log_{10}\left(\dfrac{d}{R_{bp}}\right) & \text{for} \quad d \le R_{bp} \\ 40 \log_{10}\left(\dfrac{d}{R_{bp}}\right) & \text{for} \quad d > R_{bp} \end{cases} \tag{3}$$

L_{bp} is a value for the basic transmission loss at the break point, defined as:

$$L_{bp} = \left| 20 \log_{10}\left(\frac{\lambda^2}{8 \pi h_1 h_2}\right) \right| \tag{4}$$

The upper bound has the fading margin of 20 dB. In equation (3), the attenuation coefficient before the breakpoint is set to 2.5 because a short distance leads to a weak shadowing effect.

According to the free-space loss curve, a median value $L_{LoS,m}$ is given by:

$$L_{LoS,m} = L_{bp} + 6 + \begin{cases} 20 \log_{10}\left(\dfrac{d}{R_{bp}}\right) & \text{for} \quad d \le R_{bp} \\ 40 \log_{10}\left(\dfrac{d}{R_{bp}}\right) & \text{for} \quad d > R_{bp} \end{cases} \tag{5}$$

SHF propagation up to 15 GHz

At SHF, for path lengths up to about 1 km, road traffic will influence the effective road height and will thus affect the breakpoint distance. This distance, R_{bp}, is estimated by:

$$R_{bp} = 4\frac{(h_1 - h_s)(h_2 - h_s)}{\lambda} \tag{6}$$

where h_s is the effective road height due to such objects as vehicles on the road and pedestrians near the roadway. Hence h_s depends on the traffic on the road. The h_s values given in Tables 4 and 5 are derived from daytime and night-time measurements, corresponding to heavy and light traffic conditions, respectively. Heavy traffic corresponds to 10-20% of the roadway covered with vehicles, and 0.2-1% of the footpath occupied by pedestrians. Light traffic is 0.1-0.5% of the roadway and less than 0.001% of the footpath occupied. The roadway is 27 m wide, including 6 m wide footpaths on either side.

TABLE 4

The effective height of the road, h_s (heavy traffic)

Frequency (GHz)	**h_1 (m)**	**h_s (m)**	
		h_2 = 2.7	**h_2 = 1.6**
3.35	4	1.3	(2)
	8	1.6	(2)
8.45	4	1.6	(2)
	8	1.6	(2)
15.75	4	1.4	(2)
	8	(1)	(2)

(1) The breakpoint is beyond 1 km.

(2) No breakpoint exists.

TABLE 5

The effective height of the road, h_s (light traffic)

Frequency (GHz)	h_1 (m)	h_s (m)	
		$h_2 = 2.7$	$h_2 = 1.6$
3.35	4	0.59	0.23
	8	(1)	(1)
8.45	4	(2)	0.43
	8	(2)	(1)
15.75	4	(2)	0.74
	8	(2)	(1)

(1) No measurements taken.

(2) The breakpoint is beyond 1 km.

When h_1, $h_2 > h_s$, the approximate values of the upper and lower bounds of basic transmission loss for the SHF frequency band can be calculated using equations (1) and (3), with L_{bp} given by:

$$L_{bp} = \left| 20 \log_{10} \left\{ \frac{\lambda^2}{8\pi (h_1 - h_s)(h_2 - h_s)} \right\} \right| \tag{7}$$

On the other hand, when $h_1 \leq h_s$ or $h_2 \leq h_s$ no breakpoint exists. When two terminals are close ($d < R_s$), the basic propagation loss is similar to that of the UHF range. When two terminals are far, the propagation characteristic is such that the attenuation coefficient is cubed. Therefore, the approximate lower bound for $d \geq R_s$ is given by:

$$L_{LoS,l} = L_s + 30 \log_{10} \left(\frac{d}{R_s} \right) \tag{8}$$

The approximate upper bound for $d \geq R_s$ is given by:

$$L_{LoS,u} = L_s + 20 + 30 \log_{10} \left(\frac{d}{R_s} \right) \tag{9}$$

The basic propagation loss L_s is defined as:

$$L_s = \left| 20 \log_{10} \left(\frac{\lambda}{2\pi R_s} \right) \right| \tag{10}$$

R_s in equations (8) to (10) has been experimentally determined to be 20 m.

Based on measurements, a median value is given by:

$$L_{LoS,m} = L_s + 6 + 30\log_{10}\left(\frac{d}{R_s}\right) \qquad (11)$$

Millimetre-wave propagation

At frequencies above about 10 GHz, the breakpoint distance R_{bp} in equation (2) is far beyond the expected maximum cell radius (500 m). This means that no fourth-power law is expected in this frequency band. Hence the power distance decay-rate will nearly follow the free-space law with a path-loss exponent of about 2.2. Attenuation by atmospheric gases and by rain must also be considered.

Gaseous attenuation can be calculated from Recommendation ITU-R P.676, and rain attenuation from Recommendation ITU-R P.530.

4.1.2 NLoS situations

This situation is depicted as the paths between D and E in Fig. 1.

4.1.2.1 Frequency range from 800 to 2 000 MHz

For NLoS2 situations where both antennas are below roof-top level, diffracted and reflected waves at the corners of the street crossings have to be considered (see Fig. 3).

$$L_{NLoS2} = -10\log_{10}\left(10^{-L_r/10} + 10^{-L_d/10}\right) \quad \text{dB} \qquad (12)$$

where:

L_r: reflection path loss defined by:

$$L_r = 20\log_{10}(x_1 + x_2) + x_1 x_2 \frac{f(\alpha)}{w_1 w_2} + 20\log_{10}\left(\frac{4\pi}{\lambda}\right) \quad \text{dB} \qquad (13)$$

where:

$$f(\alpha) = \frac{3.86}{\alpha^{3.5}} \quad \text{dB} \qquad (14)$$

where $0.6 < \alpha$ [rad] $< \pi$.

L_d: diffraction path loss defined by:

$$L_d = 10\log_{10}\left[x_1 x_2 (x_1 + x_2)\right] + 2D_a - 0.1\left(90 - \alpha\frac{180}{\pi}\right) + 20\log_{10}\left(\frac{4\pi}{\lambda}\right) \quad \text{dB} \qquad (15)$$

$$D_a = \left(\frac{40}{2\pi}\right)\left[\arctan\left(\frac{x_2}{w_2}\right) + \arctan\left(\frac{x_1}{w_1}\right) - \frac{\pi}{2}\right] \quad \text{dB} \qquad (16)$$

4.1.2.2 Frequency range from 2 to 16 GHz

The propagation model for the NLoS2 situations as described in § 3.1.2 with the corner angle $\alpha = \pi/2$ rad is derived based on measurements at a frequency range from 2 to 16 GHz, where h_1, $h_2 < h_r$ and w_2 is up to 10 m (or sidewalk). The path loss characteristics can be divided into two parts: the corner loss region and the NLoS region. The corner loss region extends for d_{corner} from the point which is 1 m down the edge of the LoS street into the NLoS street. The corner loss (L_{corner}) is expressed as the additional attenuation over the distance d_{corner}. The NLoS region lies beyond the corner loss region, where a coefficient parameter (β) applies. This is illustrated by the typical curve shown in Fig. 4. Using x_1, x_2, and w_1, as shown in Fig. 3, the overall path loss (L_{NLoS2}) beyond the corner region ($x_2 > w_1/2 + 1$) is found using:

$$L_{NLoS\ 2} = L_{LoS} + L_c + L_{att} \tag{17}$$

$$L_c = \begin{cases} \dfrac{L_{corner}}{\log_{10}(1 + d_{corner})} \log_{10}(x_2 - w_1/2) & w_1/2 + 1 < x_2 \le w_1/2 + 1 + d_{corner} \\ L_{corner} & x_2 > w_1/2 + 1 + d_{corner} \end{cases} \tag{18}$$

$$L_{att} = \begin{cases} 10\beta \log_{10}\left(\dfrac{x_1 + x_2}{x_1 + w_1/2 + d_{corner}}\right) & x_2 > w_1/2 + 1 + d_{corner} \\ 0 & x_2 \le w_1/2 + 1 + d_{corner} \end{cases} \tag{19}$$

where L_{LoS} is the path loss in the LoS street for x_1 (> 20 m), as calculated in § 4.1. In equation (18), L_{corner} is given as 20 dB in an urban environment and 30 dB in a residential environment. And d_{corner} is 30 m in both environments. In equation (19), β is given by 6 in both environments.

FIGURE 4

Typical trend of propagation along street canyons with low station height for frequency range from 2 to 16 GHz

Relative signal level

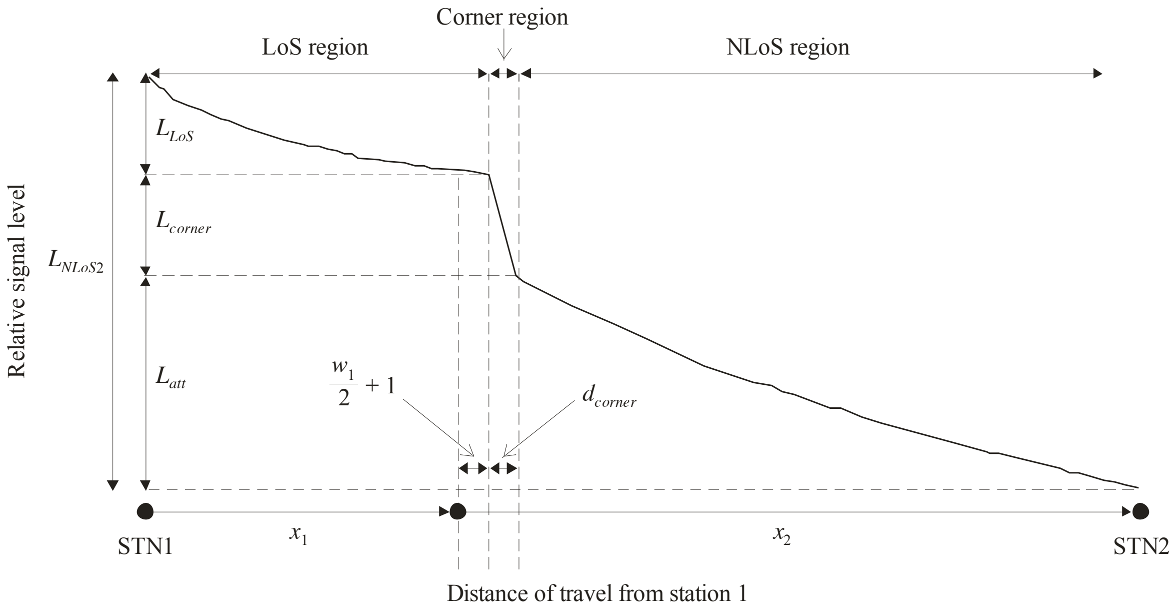

P.1411-04

In a residential environment, the path loss does not increase monotonically with distance, and thus the coefficient parameter may be lower than the value in an urban environment, owing to the presence of alleys and gaps between the houses.

With a high base station antenna in the small macro-cell, the effects of diffraction over roof-tops are more significant. Consequently, the propagation characteristics do not depend on the corner loss.

4.2 Models for propagation over roof-tops

NLoS signals can arrive at the station by diffraction mechanisms or by multipath which may be a combination of diffraction and reflection mechanisms. This section develops models that relate to diffraction mechanisms.

Propagation for urban area

Models are defined for the paths A (h_1) to B (h_2) and D (h_1) to B (h_2) as depicted in Fig. 1. The models are valid for:

h_1: 4 to 50 m

h_2: 1 to 3 m

f: 800 to 5 000 MHz

2 to 16 GHz for $h_1 < h_r$ and $w_2 < 10$ m (or sidewalk)

d: 20 to 5 000 m.

(Note that although the model is valid up to 5 km, this Recommendation is intended for distances only up to 1 km.)

Propagation for suburban area

Model is defined for the path A (h_1) to B (h_2) as depicted in Fig. 1. The model is valid for:

h_r: any height m

Δh_1: 1 to 100 m

Δh_2: 4 to 10 (less than h_r) m

h_1: $h_r + \Delta h_1$ m

h_2: $h_r - \Delta h_2$ m

f: 0.8 to 20 GHz

w: 10 to 25 m

d: 10 to 5 000 m

(Note that although the model is valid up to 5 km, this Recommendation is intended for distances only up to 1 km.)

Millimetre-wave propagation

Millimetre-wave signal coverage is considered only for LoS situations because of the large diffraction losses experienced when obstacles cause the propagation path to become NLoS. For NLoS situations, multipath reflections and scattering will be the most likely signal propagation method.

4.2.1 Urban area

The multi-screen diffraction model given below is valid if the roof-tops are all about the same height. Assuming the roof-top heights differ only by an amount less than the first Fresnel-zone radius over a path of length l (see Fig. 2), the roof-top height to use in the model is the average roof-top height. If the roof-top heights vary by much more than the first Fresnel-zone radius, a preferred method is to use the highest buildings along the path in a knife-edge diffraction calculation, as described in Recommendation ITU-R P.526, to replace the multi-screen model.

In the model for transmission loss in the NLoS1-case (see Fig. 2) for roof-tops of similar height, the loss between isotropic antennas is expressed as the sum of free-space loss, L_{bf}, the diffraction loss from roof-top to street L_{rts} and the reduction due to multiple screen diffraction past rows of buildings, L_{msd}.

In this model L_{bf} and L_{rts} are independent of the station antenna height, while L_{msd} is dependent on whether the station antenna is at, below or above building heights.

$$L_{NLoS1} = \begin{cases} L_{bf} + L_{rts} + L_{msd} & \text{for} \quad L_{rts} + L_{msd} > 0 \\ L_{bf} & \text{for} \quad L_{rts} + L_{msd} \le 0 \end{cases} \tag{20}$$

The free-space loss is given by:

$$L_{bf} = 32.4 + 20\log_{10}(d/1\,000) + 20\log_{10}(f) \tag{21}$$

where:

d: path length (m)

f: frequency (MHz).

The term L_{rts} describes the coupling of the wave propagating along the multiple-screen path into the street where the mobile station is located. It takes into account the width of the street and its orientation.

$$L_{rts} = -8.2 - 10\log_{10}(w) + 10\log_{10}(f) + 20\log_{10}(\Delta h_2) + L_{ori} \tag{22}$$

$$L_{ori} = \begin{cases} -10 + 0.354\varphi & \text{for} \quad 0° \le \varphi < 35° \\ 2.5 + 0.075(\varphi - 35) & \text{for} \quad 35° \le \varphi < 55° \\ 4.0 - 0.114(\varphi - 55) & \text{for} \quad 55° \le \varphi \le 90° \end{cases} \tag{23}$$

where:

$$\Delta h_2 = h_r - h_2 \tag{24}$$

L_{ori} is the street orientation correction factor, which takes into account the effect of roof-top-to-street diffraction into streets that are not perpendicular to the direction of propagation (see Fig. 2).

The multiple screen diffraction loss from Station 1 due to propagation past rows of buildings depends on the antenna height relative to the building heights and on the incidence angle. A criterion for grazing incidence is the "settled field distance", d_s:

$$d_s = \frac{\lambda d^2}{\Delta h_1^2} \tag{25}$$

where (see Fig. 2):

$$\Delta h_1 = h_1 - h_r \tag{26}$$

For the calculation of L_{msd}, d_s is compared to the distance l over which the buildings extend. The calculation for L_{msd} uses the following procedure to remove any discontinuity between the different models used when the length of buildings is greater or less than the "settled field distance".

The overall multiple screen diffraction model loss is given by:

$$L_{msd} = \begin{cases} -\tanh\left(\dfrac{\log(d)-\log(d_{bp})}{\chi}\right)\cdot\left(L1_{msd}(d)-L_{mid}\right)+L_{mid} & \text{for } l > d_s \text{ and } dh_{bp} > 0 \\ \tanh\left(\dfrac{\log(d)-\log(d_{bp})}{\chi}\right)\cdot\left(L2_{msd}(d)-L_{mid}\right)+L_{mid} & \text{for } l \le d_s \text{ and } dh_{bp} > 0 \\ L2_{msd}(d) & \text{for } \quad dh_{bp} = 0 \\ L1_{msd}(d)-\tanh\left(\dfrac{\log(d)-\log(d_{bp})}{\zeta}\right)\cdot\left(L_{upp}-L_{mid}\right)-L_{upp}+L_{mid} & \text{for } l > d_s \text{ and } dh_{bp} < 0 \\ L2_{msd}(d)+\tanh\left(\dfrac{\log(d)-\log(d_{bp})}{\zeta}\right)\cdot\left(L_{mid}-L_{low}\right)+L_{mid}-L_{low} & \text{for } l \le d_s \text{ and } dh_{bp} < 0 \end{cases} \tag{27}$$

where:

$$dh_{bp} = L_{upp} - L_{low} \tag{28}$$

$$\zeta = (L_{upp} - L_{low}) \cdot \upsilon \tag{29}$$

$$L_{mid} = \frac{(L_{upp} + L_{low})}{2} \tag{30}$$

$$L_{upp} = L1_{msd}(d_{bp}) \tag{31}$$

$$L_{low} = L2_{msd}(d_{bp}) \tag{32}$$

and

$$d_{bp} = |\Delta h_1|\sqrt{\frac{1}{\lambda}} \tag{33}$$

$$\upsilon = [0.0417]$$

$$\chi = [0.1]$$

where the individual model losses, $L1_{msd}(d)$ and $L2_{msd}(d)$, are defined as follows:

Calculation of $L1_{msd}$ for $l > d_s$

(Note this calculation becomes more accurate when $l >> d_s$.)

$$L1_{msd}(d) = L_{bsh} + k_a + k_d \log_{10}(d/1\,000) + k_f \log_{10}(f) - 9\log_{10}(b) \tag{34}$$

where:

$$L_{bsh} = \begin{cases} -18\log_{10}(1+\Delta h_1) & \text{for} \quad h_1 > h_r \\ 0 & \text{for} \quad h_1 \le h_r \end{cases} \tag{35}$$

is a loss term that depends on the antenna height:

$$k_a = \begin{cases} 71.4 & \text{for} \quad h_1 > h_r \text{ and } f > 2\,000 \text{ MHz} \\ 73 - 0.8\Delta h_1 & \text{for} \quad h_1 \le h_r,\ f > 2\,000 \text{ MHz and } d \ge 500 \text{ m} \\ 73 - 1.6\Delta h_1\ d/1\,000 & \text{for} \quad h_1 \le h_r,\ f > 2\,000 \text{ MHz and } d < 500 \text{ m} \\ 54 & \text{for} \quad h_1 > h_r \text{ and } f \le 2\,000 \text{ MHz} \\ 54 - 0.8\Delta h_1 & \text{for} \quad h_1 \le h_r,\ f \le 2\,000 \text{ MHz and } d \ge 500 \text{ m} \\ 54 - 1.6\Delta h_1\ d/1\,000 & \text{for} \quad h_1 \le h_r,\ f \le 2\,000 \text{ MHz and } d < 500 \text{ m} \end{cases} \tag{36}$$

$$k_d = \begin{cases} 18 & \text{for} \quad h_1 > h_r \\ 18 - 15\dfrac{\Delta h_1}{h_r} & \text{for} \quad h_1 \le h_r \end{cases} \tag{37}$$

$$k_f = \begin{cases} -8 & \text{for} \quad f > 2\,000 \text{ MHz} \\ -4 + 0.7(f/925 - 1) & \text{for medium sized city and suburban} \\ & \text{centres with medium tree density and } f \le 2\,000 \text{ MHz} \\ -4 + 1.5(f/925 - 1) & \text{for metropolitan centres and } f \le 2\,000 \text{ MHz} \end{cases} \tag{38}$$

Calculation of $L2_{msd}$ for $l < d_s$

In this case a further distinction has to be made according to the relative heights of the antenna and the roof-tops:

$$L2_{msd}(d) = -10\log_{10}\left(Q_M^2\right) \tag{39}$$

where:

$$Q_M = \begin{cases} 2.35\left(\dfrac{\Delta h_1}{d}\sqrt{\dfrac{b}{\lambda}}\right)^{0.9} & \text{for} \quad h_1 > h_r + \delta h_u \\ \dfrac{b}{d} & \text{for} \quad h_1 \le h_r + \delta h_u \text{ and } h_1 \ge h_r + \delta h_l \\ \dfrac{b}{2\pi d}\sqrt{\dfrac{\lambda}{\rho}}\left(\dfrac{1}{\theta} - \dfrac{1}{2\pi + \theta}\right) & \text{for} \quad h_1 < h_r + \delta h_l \end{cases} \tag{40}$$

and

$$\theta = \arctan\left(\frac{\Delta h_1}{b}\right) \tag{41}$$

$$\rho = \sqrt{\Delta h_1^2 + b^2} \tag{42}$$

and

$$\delta h_u = 10^{-\log_{10}\left(\sqrt{\frac{b}{\lambda}}\right) - \frac{\log_{10}(d)}{9} + \frac{10}{9}\log_{10}\left(\frac{b}{2.35}\right)} \tag{43}$$

$$\delta h_l = \frac{0.00023b^2 - 0.1827b - 9.4978}{(\log_{10}(f))^{2.938}} + 0.000781b + 0.06923 \tag{44}$$

4.2.2 Suburban area

A propagation model for the NLoS1-Case based on geometrical optics (GO) is shown in Fig. 2. This figure indicates that the composition of the arriving waves at Station 2 changes according to the Station 1-Station 2 distance. A direct wave can arrive at Station 2 only when the Station 1-Station 2 distance is very short. The several-time (one-, two-, or three-time) reflected waves, which have a relatively strong level, can arrive at Station 2 when the Station 1-Station 2 separation is relatively short. When the Station 1-Station 2 separation is long, the several-time reflected waves cannot arrive and only many-time reflected waves, which have weak level beside that of diffracted waves from building roofs, arrive at Station 2. Based on these propagation mechanisms, the loss due to the distance between isotropic antennas can be divided into three regions in terms of the dominant arrival waves at Station 2. These are the direct wave, reflected wave, and diffracted wave dominant regions. The loss in each region is expressed as follows based on GO.

$$L_{NLoS1} = \begin{cases} 20 \cdot \log_{10}\left(\frac{4\pi d}{\lambda}\right) & \text{for } d < d_0 & \text{(Direct wave dominant region)} \\ L_{0n} & \text{for } d_0 \le d < d_{RD} & \text{(Reflected wave dominant region)} \\ 32.1 \cdot \log_{10}\left(\frac{d}{d_{RD}}\right) + L_{d_{RD}} & \text{for } d \ge d_{RD} & \text{(Diffracted wave dominant region)} \end{cases} \tag{45}$$

where:

$$L_{0n} = \begin{cases} L_{d_k} + \frac{L_{d_{k+1}} - L_{d_k}}{d_{k+1} - d_k} \cdot (d - d_k) & \text{when} \quad d_k \le d < d_{k+1} < d_{RD} \\ & (k = 0, 1, 2...) \\ L_{d_k} + \frac{L_{d_{RD}} - L_{d_k}}{d_{RD} - d_k} \cdot (d - d_k) & \text{when} \quad d_k \le d < d_{RD} < d_{k+1} \end{cases} \tag{46}$$

$$d_k = \frac{1}{\sin\varphi} \cdot \sqrt{B_k^2 + (h_1 - h_2)^2} \tag{47}$$

$$L_{d_k} = 20 \cdot \log_{10}\left\{\frac{4\pi d_{kp}}{0.4^k \cdot \lambda}\right\} \tag{48}$$

$$d_{RD}(f) = 0.625 \cdot (d_3 - d_1) \cdot \log_{10}(f) + 0.44 \cdot d_1 + 0.5 \cdot d_2 + 0.06 \cdot d_3 \quad (0.8\,\text{GHz} \leq f \leq 20\,\text{GHz}) \tag{49}$$

$$L_{d_{RD}} = L_{d_k} + \frac{L_{d_{k+1}} - L_{d_k}}{d_{k+1} - d_k} \cdot (d_{RD} - d_k) \qquad (d_k \leq d_{RD} \leq d_{k+1}) \tag{50}$$

$$d_{kp} = \frac{1}{\sin \varphi_k} \cdot \sqrt{A_k^2 + (h_1 - h_2)^2} \tag{51}$$

$$A_k = \frac{w \cdot (h_1 - h_2) \cdot (2k + 1)}{2 \cdot (h_r - h_2)} \tag{52}$$

$$B_k = \frac{w \cdot (h_1 - h_2) \cdot (2k + 1)}{2 \cdot (h_r - h_2)} - k \cdot w \tag{53}$$

$$\varphi_k = \tan^{-1}\left(\frac{B_k}{A_k} \cdot \tan \varphi \right) \tag{54}$$

4.3 Models for propagation between terminals located from below roof-top height to near street level

The model described below is intended for calculating the basic transmission loss between two terminals of low height in urban environments. This situation is depicted as the paths between D and F, D and E, B and E, or E and F in Fig. 1. It includes both LoS and NLoS regions, and models the rapid decrease in signal level noted at the corner between the LoS and NLoS regions. The model includes the statistics of location variability in the LoS and NLoS regions, and provides a statistical model for the corner distance between the LoS and NLoS regions. Figure 5 illustrates the LoS, NLoS and corner regions, and the statistical variability predicted by the model.

This model is recommended for propagation between low-height terminals where both terminal antenna heights are near street level well below roof-top height, but are otherwise unspecified. It is reciprocal with respect to transmitter and receiver and is valid for frequencies in the range 300-3 000 MHz. The model is based on measurements made in the UHF band with antenna heights between 1.9 and 3.0 m above ground, and transmitter-receiver distances up to 3 000 m.

FIGURE 5

Curves of basic transmission loss not exceeded for 1, 10, 50, 90 and 99% of locations (frequency = 400 MHz, suburban)

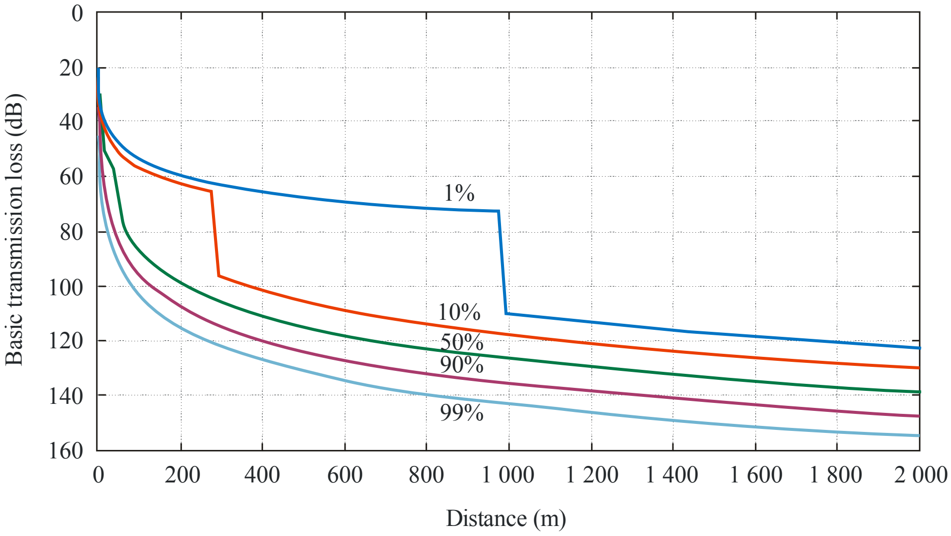

P.1411-05

The parameters required are the frequency f (MHz) and the distance between the terminals d (m).

Step 1: Calculate the median value of the line-of-sight loss:

$$L_{LoS}^{median}(d) = 32.45 + 20\log_{10} f + 20\log_{10}(d/1\,000) \tag{55}$$

Step 2: For the required location percentage, p (%), calculate the LoS location correction:

$$\Delta L_{LoS}(p) = 1.5624\sigma\left(\sqrt{-2\ln(1-p/100)} - 1.1774\right) \qquad \text{with } \sigma = 7 \text{ dB} \tag{56}$$

Alternatively, values of the LoS correction for $p = 1$, 10, 50, 90 and 99% are given in Table 6.

Step 3: Add the LoS location correction to the median value of LoS loss:

$$L_{LoS}(d,p) = L_{LoS}^{median}(d) + \Delta L_{LoS}(p) \tag{57}$$

Step 4: Calculate the median value of the NLoS loss:

$$L_{NLoS}^{median}(d) = 9.5 + 45\log_{10} f + 40\log_{10}(d/1\,000) + L_{urban} \tag{58}$$

L_{urban} depends on the urban category and is 0 dB for suburban, 6.8 dB for urban and 2.3 dB for dense urban/high-rise.

Step 5: For the required location percentage, p (%), add the NLoS location correction:

$$\Delta L_{NLoS}(p) = \sigma N^{-1}(p/100) \qquad \text{with } \sigma = 7 \text{ dB} \tag{59}$$

$N^{-1}(.)$ is the inverse normal cumulative distribution function. An approximation to this function, good for p between 1 and 99% is given by the location variability function $Q_i(x)$ of Recommendation ITU-R P.1546. Alternatively, values of the NLoS location correction for p = 1, 10, 50, 90 and 99% are given in Table 6.

TABLE 6

Table of LoS and NLoS location variability corrections

p (%)	ΔL_{LoS} (dB)	ΔL_{NLoS} (dB)	d_{LoS} (m)
1	–11.3	–16.3	976
10	–7.9	–9.0	276
50	0.0	0.0	44
90	10.6	9.0	16
99	20.3	16.3	10

Step 6: Add the NLoS location correction to the median value of NLoS loss:

$$L_{NLoS}(d,p) = L_{NLoS}^{median}(d) + \Delta L_{NLoS}(p) \tag{60}$$

Step 7: For the required location percentage, p (%), calculate the distance d_{LoS} for which the LoS fraction F_{LoS} equals p:

$$\begin{aligned} d_{LoS}(p) &= 212[\log_{10}(p/100)]^2 - 64\log_{10}(p/100) && \text{if } p < 45 \\ d_{LoS}(p) &= 79.2 - 70(p/100) && \text{otherwise} \end{aligned} \tag{61}$$

Values of d_{LoS} for p = 1, 10, 50, 90 and 99% are given in Table 6. This model has not been tested for p < 0.1%. The statistics were obtained from two cities in the United Kingdom and may be different in other countries. Alternatively, if the corner distance is known in a particular case, set $d_{LoS}(p)$ to this distance.

Step 8: The path loss at the distance d is then given as:

a) If $d < d_{LoS}$, then $L(d, p) = L_{LoS}(d, p)$

b) If $d > d_{LoS} + w$, then $L(d, p) = L_{NLoS}(d, p)$

c) Otherwise linearly interpolate between the values $L_{LoS}(d_{LoS}, p)$ and $L_{NLoS}(d_{LoS} + w, p)$:

$$\begin{aligned} L_{LoS} &= L_{LoS}(d_{LoS}, p) \\ L_{NLoS} &= L_{NLoS}(d_{LoS} + w, p) \\ L(d,p) &= L_{LoS} + (L_{NLoS} - L_{LoS})(d - d_{LoS})/w \end{aligned}$$

The width w is introduced to provide a transition region between the LoS and NLoS regions. This transition region is seen in the data and typically has a width of w = 20 m.

4.4 Default parameters for site-general calculations

If the data on the structure of buildings and roads are unknown (site-general situations), the following default values are recommended:

h_r = 3 × (number of floors) + roof-height (m)

roof-height = 3 m for pitched roofs

= 0 m for flat roofs

w = $b/2$

b = 20 to 50 m

φ = 90°.

4.5 Additional losses

4.5.1 Influence of vegetation

The effects of propagation through vegetation (primarily trees) are important for outdoor short-path predictions. Two major propagation mechanisms can be identified:

– propagation through (not around or over) trees;

– propagation over trees.

The first mechanism predominates for geometries in which both antennas are below the tree tops and the distance through the trees is small, while the latter predominates for geometries in which one antenna is elevated above the tree tops. The attenuation is strongly affected by multipath scattering initiated by diffraction of the signal energy both over and through the tree structures. For propagation through trees, the specific attenuation in vegetation can be found in Recommendation ITU-R P.833. In situations where the propagation is over trees, diffraction is the major propagation mode over the edges of the trees closest to the low antenna. This propagation mode can be modelled most simply by using an ideal knife-edge diffraction model (see Recommendation ITU-R P.526), although the knife-edge model may underestimate the field strength, because it neglects multiple scattering by tree-tops, a mechanism that may be modelled by radiative transfer theory.

4.5.2 Building entry loss

Building entry loss is the excess loss due to the presence of a building wall (including windows and other features). It is defined as the difference between the signal levels outside and inside the building at the same height. Account must also be taken of the incident angle. (When the path length is less than about 10 m, the difference in free space loss due to the change in path length for the two measurements should be taken into account in determining the building entry loss. For antenna locations close to the wall, it may also be necessary to consider near-field effects.) Additional losses will occur for penetration within the building; advice is given in Recommendation ITU-R P.1238. It is believed that, typically, the dominant propagation mode is one in which signals enter a building approximately horizontally through the wall surface (including windows), and that for a building of uniform construction the building entry loss is independent of height.

Building entry loss should be considered when evaluating the radio coverage from an outdoor system to an indoor terminal. It is also important for considering interference problems between outdoor systems and indoor systems.

The experimental results shown in Table 7 were obtained at 5.2 GHz through an external building wall made of brick and concrete with glass windows. The wall thickness was 60 cm and the window-to-wall ratio was about 2:1.

TABLE 7

Example of building entry loss

Frequency	Residential		Office		Commercial	
	Mean	Standard deviation	Mean	Standard deviation	Mean	Standard deviation
5.2 GHz			12 dB	5 dB		

Table 8 shows the results of measurements at 5.2 GHz through an external wall made of stone blocks, at incident angles from 0° to 75°. The wall was 400 mm thick, with two layers of 100 mm thick blocks and loose fill between. Particularly at larger incident angles, the loss due to the wall was extremely sensitive to the position of the receiver, as evidenced by the large standard deviation.

TABLE 8

Loss due to stone block wall at various incident angles

Incident angle (degrees)	0	15	30	45	60	75
Loss due to wall (dB)	28	32	32	38	45	50
Standard deviation (dB)	4	3	3	5	6	5

Additional information on building entry loss, intended primarily for satellite systems, can be found in Recommendation ITU-R P.679 and may be appropriate for the evaluation of building entry for terrestrial systems.

5 Multipath models

A description of multipath propagation and definition of terms are provided in Recommendation ITU-R P.1407.

5.1 Delay profile

5.1.1 Delay spread for over roof-tops propagation environments

Characteristics of multipath delay spread for both LoS and NLoS case in an urban high-rise environment for micro-cells (as defined in Table 3) have been developed based on measured data at 1 920-1 980 MHz, 2 110-2 170 MHz and 3 650-3 750 MHz using omnidirectional antennas. The median r.m.s. delay spread S in this environment is given by:

$$S_u = \exp\left(A \cdot L + B\right) \qquad \text{ns} \tag{62}$$

where both A and B are coefficients of r.m.s. delay spread and L is path loss (dB). Table 9 lists the typical values of the coefficients for distances of 100 m – 1 km based on measurements made in urban areas.

TABLE 9

Typical coefficients for r.m.s. delay spread

Measurement conditions			Coefficients of r.m.s. delay spread	
Area	**Frequency (GHz)**	**Range (m)**	**A**	**B**
Urban	3 650-3 750 MHz	100-1 000	0.031	2.091
	1 920-1 980 MHz, 2 110-2 170 MHz	100-1 000	0.038	2.3

The distributions of the multipath delay characteristics for the 3.7 GHz band in an urban environment with Station 1 antenna height of 40 m and 60 m, and Station 2 antenna height of 2 m were derived from measurements. The distributions of the multipath delay characteristics for the 3.7 GHz and 5.2 GHz band in a suburban environment with Station 1 antenna height of 20 m, and Station 2 antenna height of 2.0 m and 2.8 m were derived from measurements. Table 10 lists the measured r.m.s. delay spread for frequencies from 1.9 to 5.8 GHz for cases where the cumulative probability is 50% and 95%.

TABLE 10

Typical r.m.s. delay spread values(1), (2)

Measurement conditions						r.m.s. delay spread (ns)	
Area	**Scenario**	**Frequency (GHz)**	**Antenna height**		**Range (m)**	**50%**	**95%**
			h_1 (m)	**h_2 (m)**			
Urban-high rise(1)		1.9-2.1	46	1.7	100-1 000	490	1490
Suburban(2)		2.5	12	1	200-1 000	158	469
Urban very high-rise(1)	LoS	2.5	100	2	100-1 000	208	461
	NLoS					407	513
Urban(1)		3.7	60	2	100-1 000	232	408
			40	2	100-1 000	121	357
Suburban(1)		3.7	20	2	100-1 000	125	542
		5.2	20	2.8	100-1 000	189	577
Suburban(2)		3.5	12	1	200-1 000	161	493
		5.8	12	1	200-1 000	168	415

(1) Threshold value of 30 dB was used for r.m.s. delay spread calculation.

(2) Threshold value of 20 dB was used for r.m.s. delay spread calculation. Measurements with directional antennas at the transmitter (120° beamwidth in azimuth at 5.8 GHz and 30° at 2.5 GHz and 3.5 GHz) and omnidirectional antennas at the receiver. Time delay resolution is 100 ns.

5.1.2 Delay spread for below roof-tops propagation environments

5.1.2.1 Omnidirectional antenna case

Characteristics of multipath delay spread for the LoS omnidirectional antenna case in an urban high-rise environment for dense urban micro-cells and pico-cells (as defined in Table 3) have been developed based on measured data at frequencies from 2.5 to 15.75 GHz at distances from 50 to 400 m. The r.m.s. delay spread S at distance of d m follows a normal distribution with the mean value given by:

$$a_s = C_a d^{\gamma_a} \qquad \text{ns} \tag{63}$$

and the standard deviation given by:

$$\sigma_s = C_\sigma d^{\gamma_\sigma} \qquad \text{ns} \tag{64}$$

where C_a, γ_a, C_σ and γ_σ depend on the antenna height and propagation environment. Table 11 lists some typical values of the coefficients for distances of 50-400 m based on measurements made in urban and residential areas.

TABLE 11

Typical coefficients for the distance characteristics of r.m.s. delay spread for omnidirectional antenna case

<table>
<tr><th colspan="4">Measurement conditions</th><th colspan="2">a_s</th><th colspan="2">σ_s</th></tr>
<tr><th>Area</th><th>f (GHz)</th><th>h_1 (m)</th><th>h_2 (m)</th><th>C_a</th><th>γ_a</th><th>C_σ</th><th>γ_σ</th></tr>
<tr><td>Urban(1)</td><td>0.781</td><td>5</td><td>5</td><td>1 254.3</td><td>0.06</td><td>102.2</td><td>0.04</td></tr>
<tr><td rowspan="5">Urban(2)</td><td>2.5</td><td>6.0</td><td>3.0</td><td>55</td><td>0.27</td><td>12</td><td>0.32</td></tr>
<tr><td rowspan="2">3.35-15.75</td><td rowspan="3">4.0</td><td>2.7</td><td>23</td><td>0.26</td><td>5.5</td><td>0.35</td></tr>
<tr><td>1.6</td><td rowspan="2">10</td><td rowspan="2">0.51</td><td rowspan="2">6.1</td><td rowspan="2">0.39</td></tr>
<tr><td>3.35-8.45</td><td>0.5</td></tr>
<tr><td>8.05</td><td>5</td><td>2.5</td><td>0.97</td><td>0.78</td><td>1.42</td><td>0.52</td></tr>
<tr><td rowspan="2">Residential(2)</td><td>3.35</td><td rowspan="2">4.0</td><td>2.7</td><td>2.1</td><td>0.53</td><td>0.54</td><td>0.77</td></tr>
<tr><td>3.35-15.75</td><td>1.6</td><td>5.9</td><td>0.32</td><td>2.0</td><td>0.48</td></tr>
</table>

(1) Threshold value of 20 dB is used for r.m.s. delay spread calculation.

(2) Threshold value of 30 dB is used for r.m.s. delay spread calculation.

From the measured data at 2.5 GHz, the average shape of the delay profile was found to be:

$$P(t) = P_0 + 50\left(e^{-t/\tau} - 1\right) \qquad \text{dB} \tag{65}$$

where:

P_0: peak power (dB)

τ: decay factor

and t is in ns.

From the measured data, for an r.m.s. delay spread S, τ can be estimated as:

$$\tau = 4\,S + 266 \qquad \text{ns} \tag{66}$$

A linear relationship between τ and S is only valid for the LoS case.

From the same measurement set, the instantaneous properties of the delay profile have also been characterized. The energy arriving in the first 40 ns has a Rician distribution with a K-factor of about 6 to 9 dB, while the energy arriving later has a Rayleigh or Rician distribution with a K-factor of up to about 3 dB. (See Recommendation ITU-R P.1057 for definitions of probability distributions.)

5.1.2.2 Directional antenna case

In fixed wireless access systems and communications between the access points of wireless mesh network systems, directional antennas are employed as transmitter and receiver antennas. A typical effect of the use of directional antennas is given hereafter. Arriving delayed waves are suppressed by the antenna pattern using directional antennas as the transmitter and receiver antennas. Therefore, the delay spread becomes small. In addition, the received power increases with the antenna gain, when directional antennas are employed as the transmitter and receiver antennas. Based on these facts, the directional antenna is used in wireless systems. Therefore, it is important to understand the effect of antenna directivity in multipath models.

Characteristics of the multipath delay spread for the LoS directional antenna case in an urban high-rise environment for dense urban micro-cells and pico-cells (as defined in Table 3) were developed based on measured data in the 5.2 GHz band at distances from 10 to 500 m. The antennas were configured such that the direction of the maximum antenna gain of one antenna faced that of the other. Table 12 lists equation for deriving coefficients relative to the antenna half power beamwidth for formula (64) for distances of 10-500 m based on measurements in an urban area. These equations are only depending on the antenna half power beamwidth and effective to any width of the road.

TABLE 12

Typical coefficients for the distance characteristics of r.m.s. delay spread for directional antenna case

Measurement conditions				a_s	
Area	f **(GHz)**	h_1 **(m)**	h_2 **(m)**	C_a	γ_a
Urban	5.2	3.5	3.5	$9.3 + 1.5\log(\theta)$	$3.3 \times 10^{-2} + 4.6\theta \times 10^{-2}$

NOTE 1 – Threshold value of 20 dB is used for r.m.s. delay spread calculation.

Here, θ represents antenna half-power beamwidth at both transmitting and receiving antenna and the unit is radian. Note that θ should be set to 2π when omnidirectional antenna is applied to both transmitting and receiving antenna.

5.2 Angular profile

5.2.1 Angular spread for below roof-tops propagation environments

The r.m.s. angular spread as defined in Recommendation ITU-R P.1407 in the azimuthal direction in a dense urban micro-cell or picocell environment in an urban area was obtained from the measurement made at a frequency of 8.45 GHz. The receiving station had a parabolic antenna with a half-power beamwidth of 4°.

The measurement was also performed at the dense urban micro-cell environment in an urban area. Angular spread coefficients are introduced based on measurements in urban areas for distances of 10~1 000 m, under the LoS cases at a frequency of 0.781 GHz. Four elements omnidirectional linear array with Bartlett beam-forming method is used for deriving the angular profile.

The coefficients for r.m.s. angular spread were obtained as shown in Table 13.

TABLE 13

Typical coefficients for the distance characteristics of angular spread

Measurement conditions				**Mean (degree)**	**s.t.d (degree)**	**Remark**
Area	***f*** **(GHz)**	h_1 **(m)**	h_2 **(m)**			
Urban	0.781	5	1.5	28.15	13.98	LoS
Urban	8.45	4.4	2.7	30	11	LoS
Urban	8.45	4.4	2.7	41	18	NLoS

5.3 Number of signal components

For the design of high data rate systems with multipath separation and synthesis techniques, it is important to estimate the number of signal components (that is, a dominant component plus multipath components) arriving at the receiver. The number of signal components can be represented from the delay profile as the number of peaks whose amplitudes are within *A* dB of the highest peak and above the noise floor, as defined in Recommendation ITU-R P.1407.

5.3.1 Over-rooftops propagation environments

Table 14 shows the results for the number of signal components for over-rooftops environments from measurements in different scenarios such as type of environments, frequency bands and antenna heights.

TABLE 14

Maximum number of signal components for over-rooftops environments

Type of environment	Time delay resolution	Frequency (GHz)	Antenna height (m)		Range (m)	Maximum number of components					
						3 dB		5 dB		10 dB	
			h_1	h_2		80%	95%	80%	95%	80%	95%
Urban	200 ns	1.9-2.1	46	1.7	100-1 600	1	2	1	2	2	4
	20 ns	3.35	55	2.7	150-590	2	2	2	3	3	13
	20 ns	8.45	55	2.7	150-590	2	2	2	3	3	12
Suburban	175 ns	2.5	12	1	200-1 500	1	2	1	2	2	4
	175 ns	3.5	12	1	200-1 500	1	2	1	2	1	5
	50 ns	3.67	40	2.7	0-5 000	1	2	1	3	3	5
	100 ns	5.8	12	1	200-1 500	1	2	3	5	4	5

For the measurements described in § 5.1.1, the differential time delay window for the strongest four components with respect to the first arriving component and their relative amplitude is given in Table 15.

TABLE 15

Differential time delay window for the strongest four components with respect to the first arriving component and their relative amplitude

Type of environment	Time delay resolution	Frequency (GHz)	Antenna height (m)		Range (m)	Excess time delay (μs)							
			h_1	h_2		1st		2nd		3rd		4th	
						80%	95%	80%	95%	80%	95%	80%	95%
Urban	200 ns	1.9-2.1	46	1.7	100-1 600	0.5	1.43	1.1	1.98	1.74	2.93	2.35	3.26
Relative power with respect to strongest component (dB)						0	0	−7.3	−9	−8.5	−9.6	−9.1	−9.8

5.3.2 Below-rooftops propagation environments

Table 16 shows the results of the number of signal components for below-rooftops environments from measurements in different scenarios such as type of environments, frequency bands and antenna heights.

TABLE 16

Maximum number of signal components for below-rooftops environments

<table>
<tr><th rowspan="3">Type of environment</th><th rowspan="3">Time delay resolution</th><th rowspan="3">Frequency (GHz)</th><th colspan="2">Antenna height (m)</th><th rowspan="3">Range (m)</th><th colspan="6">Maximum number of components</th></tr>
<tr><th rowspan="2">h_1</th><th rowspan="2">h_2</th><th colspan="2">3 dB</th><th colspan="2">5 dB</th><th colspan="2">10 dB</th></tr>
<tr><th>80%</th><th>95%</th><th>80%</th><th>95%</th><th>80%</th><th>95%</th></tr>
<tr><td rowspan="3">Urban</td><td>20 ns</td><td>3.35</td><td>4</td><td>1.6</td><td>0-200
0-1 000</td><td>2
2</td><td>3
3</td><td>2
2</td><td>4
4</td><td>5
5</td><td>6
9</td></tr>
<tr><td>20 ns</td><td>8.45</td><td>4</td><td>1.6</td><td>0-200
0-1 000</td><td>1
1</td><td>3
2</td><td>2
2</td><td>3
4</td><td>4
4</td><td>6
8</td></tr>
<tr><td>20 ns</td><td>15.75</td><td>4</td><td>1.6</td><td>0-200
0-1 000</td><td>1
2</td><td>3
3</td><td>2
2</td><td>3
4</td><td>4
6</td><td>5
10</td></tr>
<tr><td>Residential</td><td>20 ns</td><td>3.35</td><td>4</td><td>2.7</td><td>0-480</td><td>2</td><td>2</td><td>2</td><td>2</td><td>2</td><td>3</td></tr>
</table>

5.4 Fading characteristics

The fading depth, which is defined as the difference between the 50% value and the 1% value in the cumulative probability of received signal levels, is expressed as a function of the product ($2\Delta f \Delta L_{max}$ MHz·m) of the received bandwidth $2\Delta f$ MHz and the maximum difference in propagation path lengths ΔL_{max} m as shown in Fig. 6. ΔL_{max} is the maximum difference in propagation path lengths between components whose level is larger than the threshold, which is 20 dB lower than the highest level of the indirect waves as shown in Fig. 7. In this figure, a in decibels is the power ratio of the direct to the sum of indirect waves, and $a = -\infty$ dB represents a NLoS situation. When $2\Delta f \Delta L_{max}$ is less than 10 MHz·m, the received signal levels in LoS and NLoS situations follow Rayleigh and Nakagami-Rice distributions, corresponding to a narrow-band fading region. When it is larger than 10 MHz·m, it corresponds to a wideband fading region, where the fading depth becomes smaller and the received signal levels follow neither Rayleigh nor Nakagami-Rice distributions.

FIGURE 6

Relationship between fading depth and $2\Delta f \Delta L_{max}$

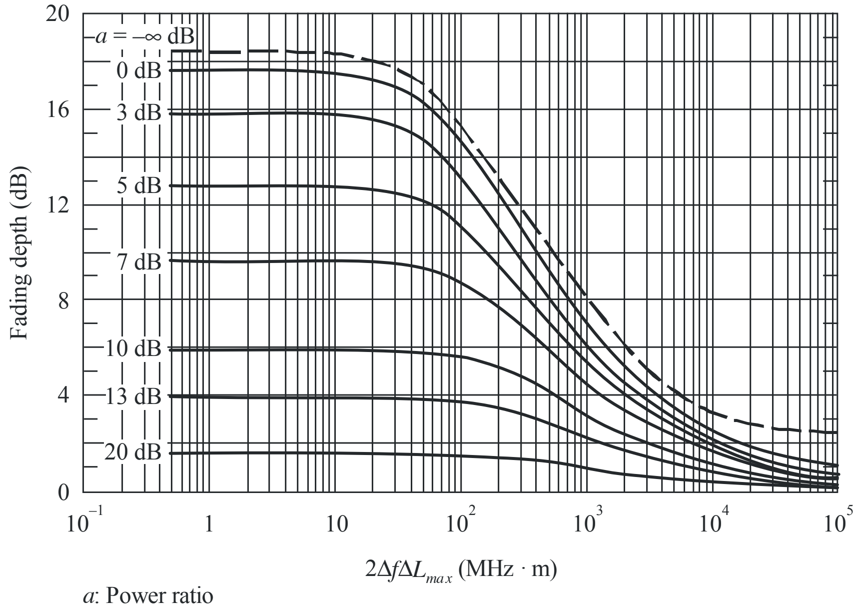

P.1411-06

FIGURE 7

Model for calculating ΔL_{max}

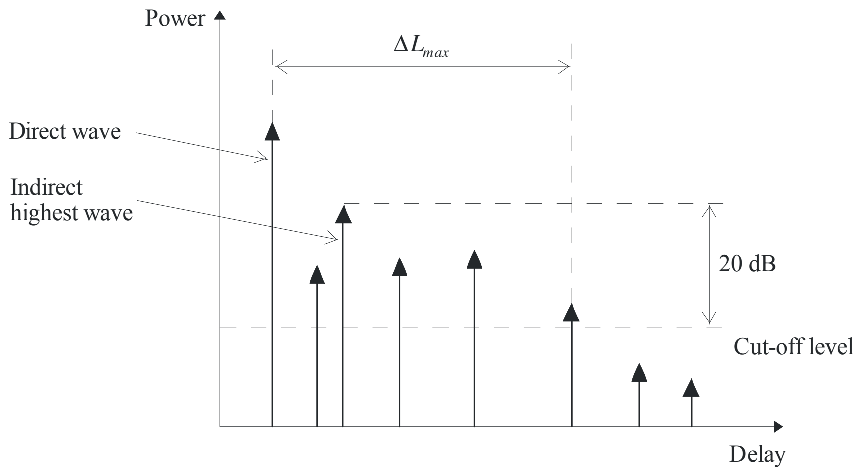

P.1411-07

6 Polarization characteristics

Cross-polarization discrimination (XPD), as defined in Recommendation ITU-R P.310, differs between LoS and NLoS areas in an SHF dense urban micro-cellular environment. Measurements indicate a median XPD of 13 dB for LoS paths and 8 dB for NLoS paths, and a standard deviation of 3 dB for LoS paths and 2 dB for NLoS paths at SHF. These median values are compatible with the UHF values for open and urban areas, respectively, in Recommendation ITU-R P.1406.

7 Propagation data and prediction methods for the path morphology approach

7.1 Classification of path morphology

In the populating area except rural area, the path morphology for wireless channels can be classified into 9 categories as shown in Table 17. The classification is fully based on real wave-propagation environment, by analysing building height and density distribution for various representative locations using GIS (Geographic Information System) database.

TABLE 17

Classification of path morphologies for the MIMO channel

Path morphology		**density**
High rise (above 25 m)	High density (HRHD)	above 35%
	Middle density (HRMD)	20 ~ 35%
	Low density (HRLD)	below 20%
Middle rise (12 m ~ 25 m)	High density (HRHD)	above 35%
	Middle density (HRMD)	20 ~ 35%
	Low density (HRLD)	below 20%
Low rise (below 12 m)	High density (HRHD)	above 35%
	Middle density (HRMD)	20 ~ 35%
	Low density (HRLD)	below 20%

7.2 Statistical modelling method

Usually the measurement data are very limited and not comprehensive. Therefore, for specific morphologies and specific operating frequencies, the following method can be used to derive the parameters for the MIMO channel model. Measurements of channel characteristics for 9 typical morphologies at 3.705 GHz have shown good statistical agreement when compared against modelling method.

Models are defined for the situation of $h_1 > h_r$. Definitions of the parameters f, d, h_r, h_1, Δh_1 and h_2 are described in Fig. 2, and B_d represents building density. The path morphology approach is valid for:

f: 800 to 6 000 MHz

d: 100 to 800 m

h_r: 3 to 60 m

h_1: $h_r + \Delta h_1$

Δh_1: up to 20 m

h_2: 1 to 3 m

B_d: 10 to 45%

In the statistical modelling, the buildings are generated in a fully random fashion. It is well known that the distribution of building height h is well fitted statistically by Rayleigh distribution $P(h)$ with the parameter μ.

$$P(h) = \frac{h}{\mu^2}\exp(\frac{-h^2}{2\mu^2}) \tag{67}$$

To derive the statistical parameters of the Rayleigh distribution for a given morphology, the use of available GIS database is recommended. For the horizontal positions of buildings, it can be assumed to be uniformly distributed.

The wave-propagation calculation is performed for each realization of building distribution using the ray tracing method. 15 times reflection and 2 times diffraction are recommended for simulation. Penetration through buildings is also important. It is recommended to set up the receiving power threshold properly to consider the building penetration. To obtain the model parameters, simulations should be performed for enough number of realizations for each morphology. At least 4 times realization is recommended. For each realization, enough number of receivers should be put in the calculation region, in order to obtain statistically meaningful data. It is recommended that at least 50 receivers are available at each 10 m sub-interval of distance. The transmitting antenna height and the receiving antenna should be set at the appropriate values. It is recommended that the values of dielectric constant and conductivity are set at $\varepsilon_r = 7.0$, $\sigma = 0.015$ S/m for buildings, and $\varepsilon_r = 2.6$, $\sigma = 0.012$ S/m for grounds.

The parameter values of building height distribution for typical cases are given in Table 18. Building sizes are 30 × 20 m^2, 25 × 20 m^2, and 20 × 20 m^2 for high, middle and low rise. Building densities are 40%, 30%, and 20% for high, middle and low density.

TABLE 18

Parameters of building height distribution for statistical modelling

Path morphology	**Rayleigh parameter μ**	**Range of building height distribution (m)**	**Average building height (m)**
HRHD	18	12.3~78.6	34.8
HRMD		12.5~70.8	34.4
HRLD		13.2~68.0	34.2
MRHD	10	7.3~41.2	19.5
MRMD		7.2~39.0	19.6
MRLD		7.4~40.4	19.4
LRHD	6	2.1~23.1	9.1
LRMD		2.5~22.2	9.4
LRLD		2.5~23.5	9.5

7.3 Path loss model

The path loss model in this Recommendation is given by:

$$PL = PL_0 + 10 \cdot n \cdot \log_{10}(d) + S \qquad \text{(dB)} \tag{68}$$

$$PL_0 = -27.5 + 20 \cdot \log_{10}(f) \qquad \text{(dB)} \tag{69}$$

where n is the path loss exponent. S is a random variable representing the random scatter around the regression line with normal distribution, and the standard deviation of S is denoted as σ_s. The units of f and d are MHz and metres, respectively.

The path loss parameters for typical cases of 9 path morphologies from statistical modelling at 3.705 GHz are summarized in Table 19. The values in the Table are fitted for all receivers at the height of 2 m located along the path at distances from 100 m to 800 m.

TABLE 19

Path loss parameters for 9 path morphologies at 3.705 GHz

Path morphology	**Transmitting antenna height (m)**	**Average building density (%)**	***n***	σ_s
HRHD	50	40	3.3	9.3
HRMD	50	30	2.9	6.3
HRLD	50	20	2.5	3.6
MRHD	30	40	2.8	4.7
MRMD	30	30	2.6	4.9
MRLD	30	20	2.3	2.7
LRHD	20	40	2.4	1.3
LRMD	20	30	2.3	1.8
LRLD	20	20	2.2	1.8

7.4 Delay spread model

The r.m.s. delay spread can also be modelled as a function of distance. The r.m.s. delay spread along NLoS-dominant paths at distances from 100 m to 800 m can be modelled as a distance-dependent model given by:

$$DS = A \cdot d^B \qquad \text{(ns)} \qquad (70)$$

The delay spread parameters for typical cases of 9 path morphologies from statistical modelling at 3.705 GHz are summarized in Table 20. The receiver heights are 2 m, and outliers are properly removed to obtain the fitted parameters.

TABLE 20

Delay spread parameters for 9 path morphologies at 3.705 GHz

Path morphology	Transmitting antenna height (m)	Average building density (%)	Delay spread (ns)	
			A	*B*
HRHD	50	40	237	0.072
HRMD	50	30	258	0.074
HRLD	50	20	256	0.11
MRHD	30	40	224	0.095
MRMD	30	30	196	0.12
MRLD	30	20	172	0.19
LRHD	20	40	163	0.18
LRMD	20	30	116	0.23
LRLD	20	20	90	0.29

7.5 Angular spread model

The angular spread of departure (ASD) and arrival (ASA) along the paths at distances from 100 m to 800 m can be modelled as a distance-dependent model given by:

$$ASD = \alpha \cdot d^{\beta} \qquad \text{(degrees)} \tag{71}$$

$$ASA = \gamma \cdot d^{\delta} \qquad \text{(degrees)} \tag{72}$$

The parameters of ASD and ASA for typical cases of 9 path morphologies from statistical modelling at 3.705 GHz are summarized in Tables 21 and 22.

TABLE 21

ASD parameters for 9 path morphologies at 3.705 GHz

Path morphology	Transmitting antenna height (m)	Average building density (%)	α	β
HRHD	50	40	107	–0.13
HRMD	50	30	116	–0.18
HRLD	50	20	250	–0.31
MRHD	30	40	115	–0.22
MRMD	30	30	232	–0.33
MRLD	30	20	264	–0.37
LRHD	20	40	192	–0.33
LRMD	20	30	141	–0.29
LRLD	20	20	113	–0.24

TABLE 22

ASA parameters for 9 path morphologies at 3.705 GHz

Path morphology	Transmitting antenna height (m)	Average building density (%)	γ	δ
HRHD	50	40	214	–0.27
HRMD	50	30	147	–0.17
HRLD	50	20	140	–0.14
MRHD	30	40	127	–0.15
MRMD	30	30	143	–0.16
MRLD	30	20	132	–0.13
LRHD	20	40	109	–0.09
LRMD	20	30	124	–0.11
LRLD	20	20	94	–0.06

8 Cross-correlation model of multi-link channel

8.1 Definition of parameters

A cross-correlation model of multi-link channel in a residential environment has been developed based on measurement data at frequency 3.7 GHz at distances from 50 to 600 m. Figure 8 depicts a geometrical diagram of multi-link channel. For geometrical modelling of the multi-link channel, the following two parameters, i.e. the angle of separation and the relative distance are used.

FIGURE 8

Diagram of multi-link

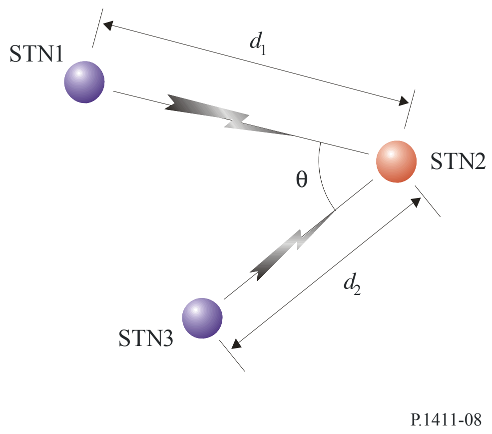

The angle of separation θ is the angle between the direct link of STN1-STN2 and the direct link of STN3-STN2. Relative distance $\tilde{d}$ is defined as:

$$\tilde{d} = \log_{10} \frac{d_1}{d_2} \tag{73}$$

where d_1 and d_2 represent respectively the distance between Station 1 and Station 2 as well as between Station 3 and Station 2. When the Station 2 is away from the Station 1 and the Station 3 with the same distance, $\tilde{d} = 0$.

The range of θ and $\tilde{d}$ are defined as,

$$0^\circ < \theta < 180^\circ, -0.3 \leq \tilde{d} \leq 0.3 \tag{74}$$

8.2 Cross-correlation of the long-term time-spatial parameters

The long-term time-spatial parameters for the cross-correlation model include:

– Shadow fading (SF)

– K-factor (KF)

– Delay spread (DS)

– Angle spread of arrival (ASA)

– Angle spread of departure (ASD).

Cross-correlation models of the long-term time-spatial parameters between the link STN1-STN2 and the link STN3-STN2 are given by the following equations.

The cross-correlation models (ρ) of SF, KF, DS, ASA and ASD between two links with respect to the angle of separation are defined as follows,

$$\rho_{(SF,KF,DS,ASA)}(\theta) = A \cdot \exp(-\theta^2/B) \tag{75}$$

$$\rho_{ASD}(\theta) = A \cdot \ln(\theta) + B \tag{76}$$

The typical coefficients of each cross-correlation model with respect to the angle of separation are obtained based on measurements in typical residential environments at 3.7 GHz respectively as shown in Table 23.

TABLE 23

Typical coefficients for cross-correlation models of the long-term time-spatial parameters with respect to the angle of separation

Parameter	Area	Frequency (GHz)	Antenna height		Cross-correlation coefficients			
			h_1 and h_3 (m)	h_2 (m)	*A*		*B*	
					mean	*s.t.d*	*mean*	*s.t.d*
Shadow fading	Residential	3.7	25	2	0.749	4.3×10^{-2}	619	89
K-factor					0.295	4.9×10^{-3}	2 129	6
Delay spread					0.67	7.0×10^{-2}	1 132	119
Angle spread of arrival					0.582	2.1×10^{-3}	1 780	484
Angle spread of departure					−0.0989	9.2×10^{-4}	0.483	0.016

The cross-correlation models (ρ) of SF, KF, DS, ASA and ASD between two links with respect to the relative distance are defined as follows:

$$\rho_{(\mathrm{SF,KF,DS,ASA})}(\tilde{d}) = A \cdot \exp(-|\tilde{d}|/B) \tag{77}$$

$$\rho_{\mathrm{ASD}}(\tilde{d}) = A \cdot |\tilde{d}| + B \tag{78}$$

The typical coefficients of each cross-correlation model with respect to the relative distance are obtained based on measurements in typical residential environments at 3.7 GHz respectively as shown in Table 24.

TABLE 24

Typical coefficients for cross-correlation models of the long-term time-spatial parameters with respect to the relative distance

Parameter	**Area**	**Frequency (GHz)**	**Antenna height**		**Cross-correlation coefficients**			
			h_1 and h_3 (m)	**h_2 (m)**	***A***		***B***	
					mean	***s.t.d***	***mean***	***s.t.d***
Shadow fading	Residential	3.7	25	2	0.572	1.4×10^{-2}	0.38	4.9×10^{-2}
K-factor					0.429	2.8×10^{-3}	0.27	7.1×10^{-3}
Delay spread					0.663	4.6×10^{-2}	0.38	1.6×10^{-1}
Angle spread of arrival					0.577	1.1×10^{-2}	0.38	2.1×10^{-2}
Angle spread of departure					0.51	1.9×10^{-1}	0.196	4.2×10^{-2}

The cross-correlation model (ρ) of SF, KF, DS, ASA and ASD between two links with respect to the angle of separation and relative distance are given by:

$$\rho_{(\mathrm{SF,KF,DS,ASA,ASD})}(\theta, \tilde{d}) = A \cdot \exp\left(-\frac{\theta^2}{B^2}\right) \cdot \exp\left(-\frac{\tilde{d}^2}{C^2}\right) \tag{79}$$

The typical coefficients of the cross-correlation model with respect to the angle of separation and relative distance are obtained based on measurements in typical residential environments at 3.7 GHz as shown in Table 25.

TABLE 25

Typical coefficients for cross-correlation model of the long-term time-spatial parameters with respect to the angle of separation and relative distance

Parameter	Area	Frequency (GHz)	Antenna height		Cross-correlation coefficients					
			h_1 and h_3 (m)	h_2 (m)	*A*		*B*		*C*	
					mean	*s.t.d*	*mean*	*s.t.d*	*mean*	*s.t.d*
Shadow fading	Residential	3.7	25	2	0.53	7.1×10^{-3}	29.31	4.6	0.42	9.2×10^{-2}
K-factor					0.28	6.4×10^{-2}	22.48	5.9	0.21	4.2×10^{-2}
Delay spread					0.46	9.2×10^{-2}	29.31	3.7	0.21	7.1×10^{-5}
Angle spread of arrival					0.49	4.9×10^{-2}	29.31	0.15	0.21	2.1×10^{-2}
Angle spread of departure					0.34	6.4×10^{-2}	29.31	2.5	0.21	2.1×10^{-2}

8.3 Cross-correlation of short-term fading in delay domain

The cross-correlation of the link STN1-STN2 channel impulse response $h_i(\tau_i)$ at the delay τ_i and the link STN3-STN2 channel impulse response $h_j(\tau_j)$ at the delay τ_j can be calculated as:

$$c_{h_ih_j}\left(\tau_i,\tau_j\right) = \mathrm{Real}\{\mathrm{E}[(\ h_i(\tau_i) - \bar{h}_i(\tau_i))(h_j(\tau_j) - \bar{h}_j(\tau_j))^*]\} \tag{80}$$

where $\overline{(\bullet)}$ represents the expectation of the given argument. Notice that only the delay samples of the channel impulse responses with power belonging to the dynamic range (5 dB) are considered to be the components for computing the cross-correlation. Furthermore, the cross-correlation coefficients, with the values from –1 to 1 are obtained by normalization, i.e.

$$c_{h_ih_j}\left(\tau_i,\tau_j\right) = \mathrm{Real}\{\frac{\mathrm{E}[(h_i(\tau_i) - \bar{h}_i(\tau_i))(h_j(\tau_j) - \bar{h}_j(\tau_j))^*]}{\sqrt{\mathrm{E}[(h_i(\tau_i) - \bar{h}_i(\tau_i))^2]}\sqrt{\mathrm{E}[(h_j(\tau_j) - \bar{h}_j(\tau_j))^2]}}\} \tag{81}$$

The following three parameters are considered for modelling the cross-correlation of short-term fading $c_{h_ih_j}(\tau_i,\tau_j)$:

– The maximum of cross-correlation of short-term fading $c_{h_ih_j}(\tau_i,\tau_j)$

$$\rho_{\mathrm{F}max} = \max\{c_{h_ih_j}(\tau_i,\tau_j)\} \tag{82}$$

– The minimum of cross-correlation of short-term fading $c_{h_ih_j}(\tau_i,\tau_j)$

$$\rho_{\mathrm{F}min} = \min\{c_{h_ih_j}(\tau_i,\tau_j)\} \tag{83}$$

– The standard deviation of cross-correlation of short-term fading $c_{h_ih_j}(\tau_i,\tau_j)$

$$\rho_{\mathrm{F}std} = \sqrt{\frac{1}{T_iT_j}\int(c_{h_ih_j}(\tau_i,\tau_j) - c_{h_ih_j,\mathrm{mean}})^2\,\mathrm{d}\tau_i\mathrm{d}\tau_j} \tag{84}$$

where T_i and T_j represent duration of τ_i and τ_j, respectively. And $c_{h_i h_j,\text{mean}}$ represents the mean value of cross-correlation of short-term fading. It is close to zero with a small variance regardless of the angle of separation and relative distance.

The cross-correlation models (ρ_F) of the small scale fading between two links with respect to the angle of separation are given by:

$$\rho_F(\theta) = A \cdot \ln(\theta) + B \tag{85}$$

The typical coefficients of each cross-correlation model with respect to the angle of separation are obtained based on measurements in typical residential environments at 3.7 GHz as shown in Table 26.

TABLE 26

Typical coefficients of cross-correlation models for the short-term fading with respect to the angle of separation

Parameter	**Area**	**Frequency (GHz)**	**Antenna height**		**Cross-correlation coefficients**			
			h_1 and h_3 (m)	**h_2 (m)**	***A***		***B***	
					mean	***s.t.d***	***mean***	***s.t.d***
Maximum	Residential	3.7	25	2	-1.09×10^{-2}	2.5×10^{-3}	0.635	3.5×10^{-3}
Minimum					1.62×10^{-2}	6.4×10^{-4}	-0.659	1.1×10^{-2}
Standard deviation					-9.71×10^{-3}	7.1×10^{-5}	0.417	7.1×10^{-5}

The cross-correlation model of short-term fading between two links with respect to the relative distance is given by:

$$\rho_F(\tilde{d}) = A \cdot \exp(-|\tilde{d}|/B) \tag{86}$$

The typical coefficients of each cross-correlation functions with respect to the relative distance are obtained based on measurements in typical residential environments at 3.7 GHz as shown in Table 27.

TABLE 27

Typical coefficients of cross-correlation model for the short-term fading with respect to the relative distance

Parameter	**Area**	**Frequency (GHz)**	**Antenna height**		**Cross-correlation coefficients**			
			h_1 and h_3 (m)	**h_2 (m)**	***A***		***B***	
					mean	***s.t.d***	***mean***	***s.t.d***
Maximum	Residential	3.7	25	2	0.628	2.8×10^{-3}	5.1	7.1×10^{-5}
Minimum					-0.626	5.7×10^{-3}	3.75	1.0×10^{-1}
Standard deviation					0.401	7.1×10^{-4}	5.1	7.1×10^{-5}